Water adsorption on clean Ni(111) and $p(2\times2)$-Ni(111)-O surfaces calculated from first principles

S. Wippermann and W. G. Schmidt
Lehrstuhl für Theoretische Physik, Universität Paderborn, 33095 Paderborn, Germany
(Received 9 August 2008; published 31 December 2008)

A systematic and comprehensive analysis of the adsorption of water monomers, small water clusters, and water thin films on clean and oxygen-predosed Ni(111) surfaces is performed. For the clean Ni surface, the formation of water hexamers (and possibly also incommensurate icelike bilayers) is favored. The total-energy results as well as the calculated vibrational frequencies for water adsorbed on the $p(2\times2)$-Ni(111)-O surface suggest a reinterpretation of recent experimental data [M. Nakamura and M. Ito, Phys. Rev. Lett. **94**, 035501 (2005)] in terms of single water monomers adsorbed on top of Ni and the formation of (islands of) an icelike bilayer.

DOI: 10.1103/PhysRevB.78.235439 PACS number(s): 68.43.Bc, 82.30.Rs

The interaction of water with solid surfaces is fundamental to research in fields as diverse as corrosion, cellular biology, and atmospheric chemistry. Despite substantial research efforts, the structural properties of water are at best incompletely understood. This holds for the ubiquitous liquid phase[1,2] as well as for thin substrate-supported water films and clusters prepared in the laboratory.[3–5] In order to explore the mutual interaction of water monomers and its modification by the substrate, the experimental and theoretical research focuses on well-defined model systems that are accessible to both advanced surface-sensitive probes and *first-principles* calculations. The adsorption of water on clean and oxygen-adsorbed Ni(111) surfaces is one example in this respect. However, the existing data do not result in a consistent picture describing the adsorption of water on the Ni surface.

Infrared (IR) data obtained from water adsorbed Ni(111) surfaces (coverage $\Theta=0.33$, i.e, one water molecule per three surface Ni atoms) were interpreted by the coexistence of water hexamers and water dimers at the surface.[6] A subsequent theoretical study[7] argued, however, that also monomer contributions are needed to explain the experimental data. On the other hand, the formation of (islands of) an icelike hexagonal hydrogen-bonded network—incommensurate to the substrate—was concluded from electron-diffraction data.[8] This was interpreted in terms of a particularly weak bonding between the water monomers and the Ni surface. First-principles calculations within density-functional theory (DFT) determined a value of 0.24 eV for the adsorption energy of a single water monomer on the Ni(111) surface.[9] Interestingly, this value was found to increase substantially (to 0.67 eV) upon dimer formation. Nakamura and Ito[10] used oxygen as anchoring atoms for water and studied the adsorption of H_2O on the $p(2\times2)$-Ni(111)-O surface using x-ray diffraction and IR reflection absorption.[11] From their data they conclude that at low temperature (25 K) the water monomers chemisorb close to the oxygen in threefold-coordinated Ni sites, with one Ni adsorbed O surrounded by one to three monomeric water molecules, while at elevated temperatures monomeric water molecules adsorb on top of the Ni atoms.

Here we present a comprehensive computational study on the structural, energetic, and vibrational properties of water molecules interacting with clean and oxygen-covered Ni(111) surfaces. The calculations are performed using DFT within the generalized gradient approach (GGA) as implemented in the Vienna *Ab initio* Simulation Package (VASP).[12] The electron-ion interaction is described by the projector-augmented wave scheme.[13] The electronic wave functions are expanded into plane waves up to a kinetic energy of 340 eV. The surface is modeled by periodically repeated slabs. Each supercell consists of six Ni layers within (4×4) or (6×6) periodicity plus the adsorbed water and (if applicable) oxygen as well as a vacuum region equivalent to six metal layers. The five Ni layers as well as the adsorbate degrees of freedom are allowed to relax until the forces on the atoms are below 20 meV/Å. The Brillouin-zone integration is performed using—depending on the surface periodicity—$6\times6\times1$ or $4\times4\times1$ Monkhorst-Pack meshes. We use the PW91 functional[14] to describe the electron exchange and correlation energy within the GGA. It describes the hydrogen bonds in solid water (ice I_h) in good agreement with experiment.[15,16] However, in the case of molecules weakly bonded to each other or to the surface, dispersion interaction—not accounted for in the GGA—may contribute a sizable percentage of the total interaction energy.[17] In order to assess at least approximately the influence of the van der Waals (vdW) interaction on the adsorption geometries and energetics, we additionally present data that are obtained using a semiempirical approach based on the London dispersion formula to include the dispersion interaction.[18] Clearly, such an approach is limited in its accuracy, in particular, if applied to metallic systems, and should be considered to provide error bars rather than accurate results.

We start by determining the potential-energy surfaces (PESs) for a single water monomer adsorbed on the clean Ni(111) and the $p(2\times2)$-Ni(111)-O surface, respectively. In order to account for the fact that energy barriers hinder the free rotation of surface-adsorbed water molecules, the minimum-energy geometry for every PES sampling point was obtained by probing different molecular starting orientations. In order to minimize the interactions with image molecules in neighboring unit cells, a (4×4) lateral periodicity was used in both cases. As can be seen in Fig. 1(a), the energy landscape experienced by water monomers on the

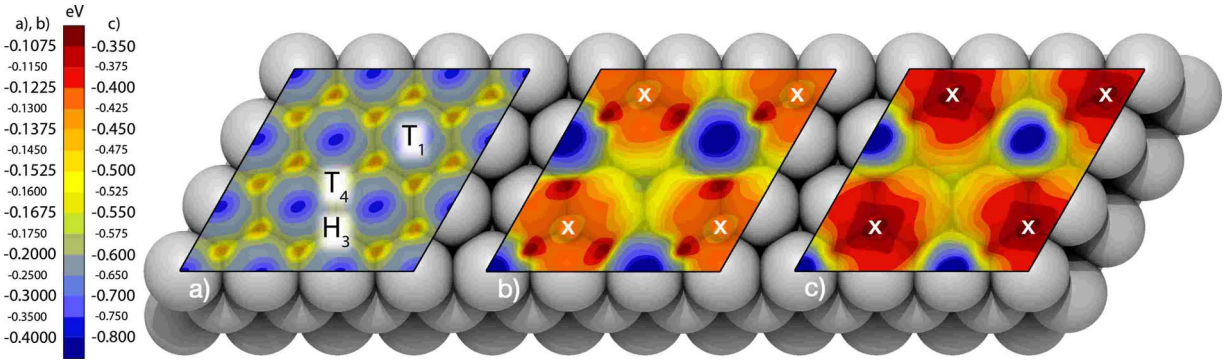

FIG. 1. (Color online) Potential-energy surfaces for a single water monomer adsorbed on the (a) clean Ni(111) surface and $p(2\times2)$-Ni(111)-O surface (b) without and (c) with vdW extension. Adsorbed oxygen atoms on the surface are marked by white crosses. The positions of the T_1, T_4, and H_3 adsorption sites are indicated.

clean Ni(111) surface is rather flat. The energy barriers that hinder the lateral movements of single water molecules are 0.24 eV. In agreement with earlier calculations,[9] the energetically most favored adsorption position is found on top of Ni surface atoms, i.e., at the T_1 site. Thereby the molecules adsorb flat, i.e., the molecular plane is parallel to the Ni surface. Compared to T_1, the adsorption on both the H_3 and T_4 sites is less favorable, $E_{ad}=-0.14$ eV compared to $E_{ad}=-0.38$ eV. Preadsorbed oxygen changes the water-surface interaction. The PES calculated for H_2O adsorbed on the $p(2\times2)$-Ni(111)-O surface is shown in Fig. 1(b). The T_1 site still represents the most favored adsorption site. The adsorption energy, however, increases to $E_{ad}=-0.6$ eV. This holds also for the energy barriers for lateral movements that now amount to at least 0.33 eV. Nakamura and Ito[10] interpreted their x-ray data for water monomers adsorbed on the $p(2\times2)$-Ni(111)-O surface in terms of molecules occupying H_3 and T_1/T_4 sites at low (25 K) and elevated (140 K) temperatures, respectively. Our total-energy results support the occupation of T_1/T_4 positions but do not give any explanation for H_2O adsorbed at H_3 sites; while the T_4 sites are shallow local minima on the PES, the H_3 sites are not even local minima. This deviation between the numerical results and the interpretation of the experimental data is not likely to be related to the neglect of van der Waals forces in the DFT calculations. The inclusion of dispersion interaction does not change the qualitative results obtained within DFT-GGA. However, as shown in Fig. 1(c), the corrugation of the PES as well as the adsorption energy increase upon inclusion of dispersion interaction.

Structural details and adsorption energies for the water monomers adsorbed on the $p(2\times2)$-Ni(111)-O surface are given in Fig. 2(a) and in Table I. Among the threefold-coordinated sites, DFT favors the flat adsorption configuration on the T_4 position, which does also hold upon inclusion of vdW corrections. However, the T_1 adsorption site remains the most favored (by about 0.4 eV) configuration irrespective of the inclusion of dispersion interaction.

In the next step we examined the adsorption of water dimers and trimers on the clean as well as the $p(2\times2)$-Ni(111)-O surface. In order to scan the available configurational space, a wide range of different starting geom-

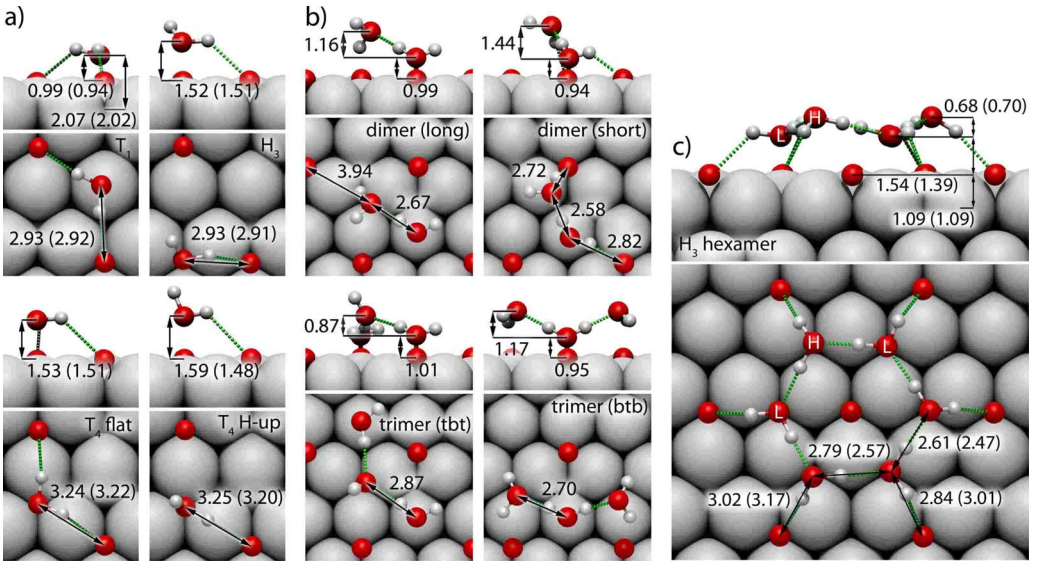

FIG. 2. (Color online) Top and side views of (a) the water monomer, (b) dimer and trimer adsorption configurations, and (c) the water hexamers formed on the $p(2\times2)$-Ni(111)-O surface. Atomic distances are given in angstroms, with vdW-corrected results in brackets.

TABLE I. Monomer and multimer adsorption energies (in eV, per molecule) on the clean Ni(111) (data with ∗) as well as the $p(2\times2)$-Ni(111)-O surface. The notation refers to Fig. 2.

	E_{ad}/H_2O (eV)	
Adsorbate system	DFT	DFT+vdW
Monomer T_1 (∗)	−0.376	
Dimer (∗)	−0.492	
Trimer *b-t-b* (∗)	−0.479	
Monomer T_1	−0.599	−0.992
Monomer H_3 H-up	−0.167	−0.495
Monomer T_4 flat	−0.171	−0.517
Monomer T_4 H-up	−0.110	−0.398
Dimer short	−0.578	
Dimer long	−0.513	
Trimer *b-t-b*	−0.542	
Trimer *t-b-t*	−0.516	

etries and orientations has been examined. For any of the dimer/trimer structures investigated we found it necessary to include at least one H_2O molecule on top of a Ni surface atom in order to obtain a stable configuration. The most favored dimer/trimer geometries on (2×2)-Ni(111)-O are shown in Fig. 2(b). Starting configurations excluding T_1 adsorbed H_2O molecules typically relax into one of the four geometries shown. The corresponding adsorption energies can be found in Table I. Remarkably, although the dimer/trimer configurations basically form only one bond to the substrate (via the molecule in T_1 position), the energy gain upon attaching additional water monomers to the atop molecule clearly exceeds the energy gain expected upon dimer formation in the gas phase, i.e., about 0.13 eV. Instead, the energy gain is nearly equivalent to the adsorption of another H_2O molecule on top of Ni. Sebastiani and Delle Site[9] reported similar findings for the clean Ni(111) surface. While for clean Ni(111) even the adsorption energy per H_2O molecule increases upon dimer/trimer formation, this is not the case for the $p(2\times2)$-Ni(111)-O surface. The preadsorption of oxygen on the nickel surface thus reduces the attractive interaction between water monomers, at least concerning the formation of dimers or trimers.

Experiment and theory indicate a pronounced tendency of water molecules to form hexamers on a number of metal surfaces.[5] Our total-energy calculations confirm this behavior for clean Ni(111). A buckled water hexamer with the water molecules positioned on top of Ni substrate atoms yields a molecular adsorption energy of about 0.52 eV, i.e., 0.14 and 0.03 eV, more than obtained upon monomer and dimer adsorptions, respectively (cf. Tables II and I).

Cyclic buckled hexamers also correspond to a local minimum of the potential-energy surface exposed by the $p(2\times2)$-Ni(111)-O surface to H_2O molecules. However, the preadsorbed oxygen atoms require a lateral shift of the water hexamers, leading to water molecules in threefold-coordinated (H_3) sites of the Ni(111) surface, as shown in Fig. 2(c). This structure is stabilized by hydrogen bonds between the three upper H_2O molecules and O adatoms. The lower water molecules are in a less favorable position to bond to the O adatoms. This results in very different OH stretching modes for the upper and lower H_2O molecules, as will be discussed later. It is interesting to note that the water

TABLE II. Hexamer and bilayer adsorption energies (in eV) on the clean Ni(111) (data with ∗) as well as the $p(2\times2)$-Ni(111)-O surface. The notation refers to Figs. 2–5.

		θ_{H_2O} (ML)	E_{ad}/H_2O (eV)	
Adsorbate system	Adsorption site		DFT	DFT+vdW
Hexamer (∗)	H_3	0.17	−0.435	−0.890
Hexamer (∗)	T_1	0.17	−0.517	−1.044
I_h-like bilayer (∗)	T_1/T_4	0.17	−0.546	−0.982
I_h-like bilayer H-up (∗)	T_1/T_4	0.50	−0.507	−1.051
I_h-like bilayer H-down (∗)	T_1/T_4	0.50	−0.568	−1.050
I_h-like bilayer H-up (∗)	T_1/T_1	0.67	−0.524	−0.975
I_h-like bilayer H-down (∗)	T_1/T_1	0.67	−0.447	−1.098
Hexamer	H_3	0.17	−0.458	−0.894
Hexamer	H_3	0.33	−0.450	−0.931
Hexamer	H_3	0.38	−0.451	−0.895
Hexamer	H_3	0.50	−0.435	−0.938
I_h-like hexamer	H_3	0.38	−0.358	−0.749
I_h-like bilayer	T_1/T_4	0.17	−0.541	−1.019
I_h-like bilayer H-up	T_1/T_4	0.33	−0.553	−1.015
I_h-like bilayer H-up	T_1/T_4	0.50	−0.551	−0.977
I_h-like bilayer H-down	T_1/T_4	0.50	−0.553	−1.095

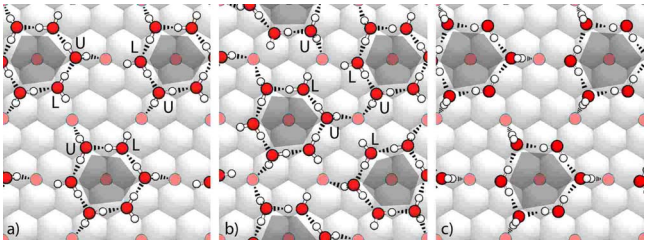

FIG. 3. (Color online) Top views of [(a) and (b)] H-bonded hexamer structures and (c) I_h-like hexamer structure of water adsorbed on the $p(2\times2)$-Ni(111)-O surface for the following coverages Θ: [(a) and (c)] 0.38 and (b) 0.5. In case of the [(a) and (b)] hexamer structure, it is energetically favorable for each surface adsorbed oxygen to accept only one H bond. However, above a coverage of 0.38 some O adatoms have to accept two H bonds, thus reducing the adsorption energy. Upper (H bonding) and lower (non-H-bonding) H_2O molecules are indicated by U and L, respectively.

hexamers feature molecules in threefold-coordinated (H_3) Ni sites, in accordance to the x-ray results obtained by Nakamura and Ito.[10] The reason for the stability of hexamers is probably related to the nearly commensurate Ni lattice. Only 27 meV per H_2O molecule is required to deform the gas-phase hexagon into the surface adsorption geometry.

Concerning the adsorption energies (cf. Table II), the calculations show that the adsorption energy increases upon formation of dimers and hexamers compared to monomeric adsorption on the clean Ni surface, while clustering is not preferred on the $p(2\times2)$-Ni(111)-O surface. Here the most favorable hexamer structure results in an adsorption energy per H_2O molecule that is 0.14 eV lower than that obtained for water monomers. This can at least partially be explained by the steric constraints caused by the O adatoms. We find the hexamer formed by molecules adsorbed in threefold-coordinated sites (as enforced by preadsorbed O) to be 0.08 eV less stable on the clean Ni surface than the minimum-energy hexamer.

In Table II also the dependence of the adsorption energy on the coverage is shown for hexameric adsorption on the $p(2\times2)$-Ni(111)-O surface. While for coverages lower than $\Theta=0.38$ the adsorption energy changes by less than 0.01 eV, it decreases for higher coverages, possibly because then some O adatoms need to accept more than one H bond [illustrated in Figs. 3(a) and 3(b)]. However, this may also be an artifact of the DFT-GGA calculations. Upon inclusion of vdW corrections the saturation coverage of $\Theta=0.5$ is the most stable one.

A further increase in the adsorption energy can be achieved, at least for the O predosed surface, if the hexamers are rotated by 30° and form an icelike bilayer, where every second H_2O molecule is adsorbed on top of Ni with the other H_2O molecules located at T_4 sites (see Figs. 4 and 5). While there are two possible configurations with the free OH bonds pointing either up or down, their adsorption energies are almost equal. Compared to the hexamer adsorption, the adsorption energy (depending on the coverage) is about 0.1 eV higher. However, it is still lower than the adsorption energy of monomeric water on top of Ni. This is different for the clean Ni(111) surface. Here the bilayer formation increases

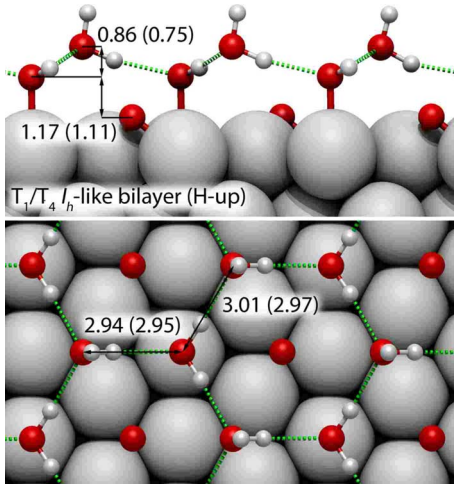

FIG. 4. (Color online) Top and side views of the hexagonal icelike (I_h) H-up bilayer structure adsorbed at T_1/T_4 sites on the $p(2\times2)$-Ni(111)-O surface. Atomic distances are given in angstroms, with vdW-corrected results in brackets.

the adsorption energy between 0.13 (H-up) and 0.19 eV (H-down) with respect to monomers. There is substantial strain involved in bilayer formation, however. We find that the equilibrium lattice constant of a gas-phase icelike bilayer is 9% smaller than that enforced by the Ni substrate. This leads to a deformation energy of about 0.09 eV (H-up) and 0.12 eV (H-down) per H_2O molecule. In case the H_2O molecules constituting the bilayer are located exclusively at T_1 sites, the gas-phase equilibrium lattice constant is 5% larger than the substrate enforced lattice constant, resulting in deformation energies of 0.02 (H-up) and 0.14 eV (H-down) per H_2O molecule, respectively. Given that the corrugation of the PES for single monomers is about 0.24 eV, this results in a subtle balance between the average bonding energy of commensurate and noncommensurate ice overlayers and may explain the experimental observation of very large $(2\sqrt{7}\times2\sqrt{7}R19°)$ surface unit cells formed by water on the clean Ni(111) surface.[8]

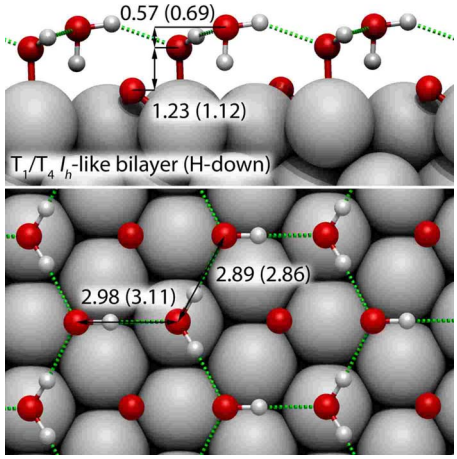

FIG. 5. (Color online) Top and side views of the hexagonal icelike (I_h) H-down bilayer structure adsorbed at T_1/T_4 sites on the $p(2\times2)$-Ni(111)-O surface. Atomic distances are given in angstroms, with vdW-corrected results in brackets.

TABLE III. Calculated phonon frequencies in cm^{-1} for D_2O adsorption configurations on the $p(2\times2)$-Ni(111)-O surface. Phonon frequencies assignable to either the higher or lower wave-number stretching modes in Fig. 6 are set in [] or {}, respectively.

Adsorbate system	Asymmetric stretching		Symmetric stretching		Bending	
I_h-like bilayer (T_1/T_4 D-up), $\theta_{D_2O}=0.5$	[2718, 2717]	T_4	{2467, 2461}	T_1/T_4	1160	T_1/T_4 antiphase
	2711, 2709	T_4	2432, 2426	T_1/T_4	1159, 1144	
	2524, 2524	T_1/T_4	2408, 2391	T_1	1141, 1136	
	2491, 2491	T_1/T_4	2385, 2377	T_1	1134	T_1/T_4 in phase
I_h-like bilayer (T_1/T_4 D-down), $\theta_{D_2O}=0.5$	2540, 2539	T_4	2382, 2375	T_1/T_4	1177	T_1/T_4 in phase
	2538, 2536	T_4	2341, 2341	T_1/T_4	1175, 1168	
	{2464, 2463}	T_1/T_4	2295, 2293	T_1	1146, 1136	
	2424, 2423	T_1/T_4	2292, 2290	T_1	1136	T_1/T_4 antiphase
Buckled hexamer (H_3), $\theta_{D_2O}=0.375$	[2719, 2710, 2692]	Lower D_2O	2130, 2096, 2053	Lower D_2O	1196	In phase
	2631, 2628, 2625	Upper D_2O	2335, 2329, 2312	Upper D_2O	1185, 1181	
					1170, 1165	
					1162	Antiphase
I_h-like hexamer (H_3 D-up), $\theta_{D_2O}=0.375$	[2732, 2731, 2729]	Upper D_2O	{2500, 2484, 2470}	Lower D_2O	1157	In phase
	2618, 2611, 2586	Lower D_2O	2433, 2428, 2413	Upper D_2O	1155, 1153	
					1150, 1137	
					1130	Antiphase
Trimer (*b-t-b*)	[2713], 2697	Upper D_2O	2597, 2577	Upper D_2O	1173	In phase
	2243	Lower D_2O	2166	Lower D_2O	1140, 1136	Antiphase
Dimer (long)	[2714]	Upper D_2O	2557	Upper D_2O	1153	In phase
	2679	Lower D_2O	2127	Lower D_2O	1134	Antiphase
Dimer (short)	[2742]	Upper D_2O	2426	Upper D_2O	1156	In phase
	2589	Lower D_2O	1943	Lower D_2O	1141	Antiphase
Monomer (H_3 D-up)	[2744]		2604		1138	
Monomer (T_4 flat)	[2735]		2609		1150	
Monomer (T_4 D-up)	2764		2625		1139	
Monomer (T_1 flat)	2643		{2519}		1128	

The adsorption of water on the $p(2\times2)$-Ni(111)-O surface has not only been characterized using x-ray diffraction but also by infrared spectroscopy.[11] In order to relate our structural models to the experimental observations, we perform frozen-phonon calculations[19] for the $H_2O/p(2\times2)$-Ni(111)-O adsorption models discussed above. The calculated frequencies (using the mass of deuterium in the calculations to be consistent with experiment) are compiled in Table III. In Fig. 6 an attempt has been made to assign the calculated frequencies to the measured IR data.

For a coverage of $\Theta=0.03$ two stretching modes at 2735 and 2519 cm^{-1} and one bending mode at 1165 cm^{-1} are observed. While both the H_3 H-up and the T_4 flat monomer yield frequencies for the asymmetric stretching mode that can explain the 2735 cm^{-1} absorption peak, among the investigated structural models the signal at 2519 cm^{-1} can only be explained by the symmetric stretching mode of the flat T_1 monomer. For the bending mode all three monomer geometries yield roughly the same frequency, but with a systematic underestimation of the measured wave number by about 30 cm^{-1}. However, the transition dipoles of the flat T_1/T_4 monomer modes are oriented almost in plane with the surface and are thus expected to show only a very weak scattering efficiency. In Ref. 11 it is argued that the bending mode is strongly coupled to a charge transfer along the water-metal bond, thereby increasing its oscillator strength, while the stretching modes exhibit no such coupling and remain almost inactive. In order to check for a possible charge transfer we calculated the charge-density difference between the equilibrium and elongated configurations for the bending and symmetric stretching mode, respectively. We did indeed observe a small charge transfer along the water-metal bond localized at the Ni atom. Additionally, another somewhat smaller charge transfer is observed at the H-bond accepting O_{ad} atoms. However, this is the case as well (with similar magnitude but slightly different directions) for both the bending and the symmetric stretching modes. In the experimental spectra of the high-temperature phase at 140 K (Ref. 11 and Fig. 5, where only monomers adsorbed at T_1/T_4 sites are expected to be present) no stretching modes and one bending mode are seen. Thus, although the structural models investigated in the present study offer no alternative explanation, the assignment of the stretching modes to flat T_1/T_4 adsorbed monomers is problematic.

In the experimental spectra of Ref. 11 and in Fig. 5 there

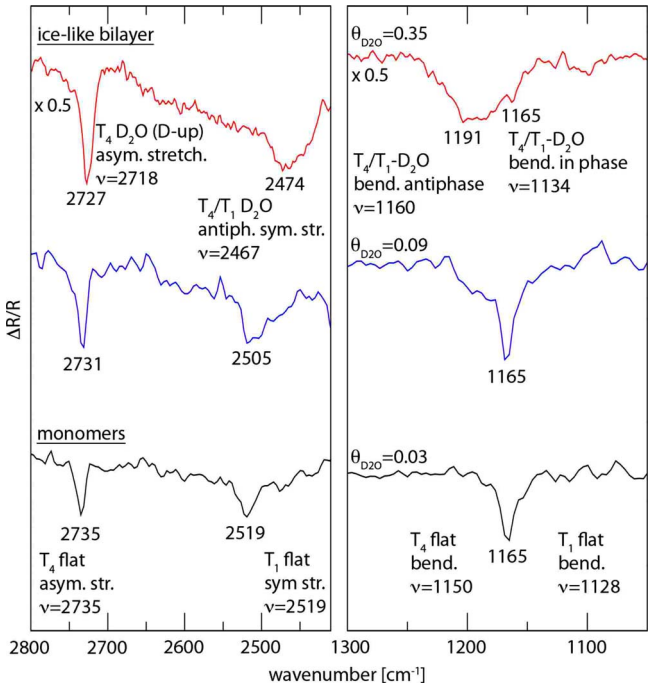

FIG. 6. (Color online) Calculated vibrational modes assigned to experimental IR spectra from Ref. 11.

is also a spectrum measured at 200 K, which exhibits a single stretching peak at 2681 cm^{-1} attributed to the formation of hydroxyls. We performed total-energy calculations for hydroxyls adsorbed on the $p(2\times2)$-Ni(111)-O surface as well. The H_3/T_4 sites are the energetically most favored adsorption sites, with the OH bond axis oriented along the surface normal. Their calculated stretching modes are located at 2666 cm^{-1} for the H_3 site and 2661 cm^{-1} for the T_4 site. These wave numbers agree well with the measured IR spectroscopy data from Ref. 11. The T_1 site is energetically less favorable and its calculated stretching mode at 2616 cm^{-1} does not agree with the available experimental data.[11] This leads us to conclude that dissociative wetting occurs on the $p(2\times2)$-Ni(111)-O surface at elevated temperatures only, with the resulting hydroxyls adsorbed at H_3/T_4 sites.

We now return to the case of nondissociated H_2O molecules. Increasing the coverage to $\Theta=0.09$ a shoulder develops at 1190 cm^{-1} that gets even more pronounced for coverages of $\Theta=0.35$. From the calculations, this can be attributed to the formation of multimers where the H_2O molecules can oscillate either in phase (higher wave number) or antiphase (lower wave number). At a coverage of 0.35 the intensities of the bending modes are fully developed, ranging from 1191 to 1165 cm^{-1}. Both the oxygen-anchored hexamers and the two icelike bilayer structures have bending modes in (or close to) this frequency range (hexamer: 1162–1196 cm^{-1}; I_h bilayer: 1134–1160 cm^{-1}). However, the stretching modes of the three structures are different and allow for further discrimination. The hexamer has two distinct stretching modes depending on the vertical positions of the constituting D_2O molecules. There are three asymmetric stretching modes from 2719–2692 cm^{-1} originating from the lower weakly H-bonded D_2O molecules. These fit well to the experimental peak at 2727 cm^{-1}. There are also three asymmetric stretching modes from the upper more strongly H-bonded D_2O molecules (2625–2631 cm^{-1}) which are not observed experimentally. Unfortunately, the symmetric stretching modes of both species (2130–2335 cm^{-1}) lie outside the range of measured frequencies. The mode at 2474 cm^{-1} cannot be explained by the hexamers but by the ice I_h-like bilayer (H-up), where symmetric stretching modes with T_4 adsorbed D-up D_2O and T_1 adsorbed flat D_2O oscillating in antiphase occur at 2461–2467 cm^{-1}. These modes can also be explained by the H-down bilayer structure, which exhibits asymmetric stretching modes at 2463–2464 cm^{-1}. However, while the H-up bilayer structure also gives rise to asymmetric stretching modes from 2709–2718 cm^{-1} that originate from the free upward pointing OD bonds of the D-up molecules, the H-down bilayer structure does not since it has no free OD bonds. Apart from the T_1/T_4 H-up I_h-bilayer structure, we found only one other structure in the present study that gives rise to all three experimentally observed modes. A single I_h bilayer such as hexamer can also be H-bond anchored at H_3 sites to the O adatoms analogous to the buckled hexamers [see Fig. 3(c)]. It exists only in H-up configuration, since the H-down I_h-like hexamer relaxes into the already discussed buckled hexamer. However, while this I_h-like hexamer exhibits the three experimentally observed modes, its adsorption energy is 0.09 eV lower than that of the buckled hexamer.

The comparison of the measured IR data with the calculated frequencies thus leads us to conclude that for low coverages monomeric water must occur, while for high coverages at least part of the surface is covered by an icelike H-up bilayer. Of course, from such a comparison the occurence of further more complex or disordered structures cannot be excluded, in particular, since no scattering efficiencies have been calculated and the present study is restricted to ordered structures. However, the conclusion that these two structures occur is consistent with calculated adsorption energies, which show a clear preferrence for the adsorption of monomers at T_1 and icelike bilayers on the $p(2\times2)$-Ni(111)-O surface.

To summarize, DFT-GGA calculations for water adsorbed on the clean and on the oxygen-adsorbed Ni(111) surface were performed. Irrespective of the existence of O adatoms, single adsorbed water molecules prefer to adsorb atop Ni substrate atoms. In case of the $p(2\times2)$-Ni(111)-O surface, however, the adsorption energy of the water monomers is higher and the corrugation of the potential-energy surface is more pronounced than for clean surfaces. For clean Ni(111) surfaces, the adsorption energy per H_2O molecule increases upon formation of dimers, trimers, and hexamers as well as icelike bilayers that are commensurate with the substrate. Given the rather shallow PES and the strain involved in the formation of commensurate overlayers, the formation of an incommensurate bilayer structure appears possible. For the $p(2\times2)$-Ni(111)-O surface, the total-energy results and the calculated vibrational frequencies suggest a reinterpretation of recent experiments in terms of single adsorbed monomers at T_1/T_4 sites for low coverages and the formation of an

H-up icelike bilayer for higher coverages, where the orientation of the bilayer is enforced by the O adatoms. The positions assumed by the water molecules in these structures are (partially) compatible with the structure model suggested from the x-ray data, while the bilayer structure itself is not.

We thank Masashi Nakamura and Masatoki Ito for providing their IR data. Financial support from the DFG as well as grants of supercomputer time by the Höchstleistungs-Rechenzentrum Stuttgart and the Paderborn Center for Parallel Computing PC^2 are gratefully acknowledged.

[1] P. Wernet, D. Nordlund, U. Bergmann, M. Cavalleri, M. Odelius, H. Ogasawara, L. Å. Naäslund, T. K. Hirsch, L. Ojamäe, P. Glatzel, L. G. M. Pettersson, and A. Nilsson, Science **304**, 995 (2004).
[2] A. Hermann, W. G. Schmidt, and P. Schwerdtfeger, Phys. Rev. Lett. **100**, 207403 (2008).
[3] P. J. Feibelman, Science **295**, 99 (2002).
[4] P. J. Feibelman, Phys. Rev. Lett. **90**, 186103 (2003).
[5] A. Michaelides and K. Morgenstern, Nature Mater. **6**, 597 (2007).
[6] M. Nakamura and M. Ito, Chem. Phys. Lett. **404**, 346 (2005).
[7] T. Murakhtina, L. Delle Site, and D. Sebastiani, ChemPhysChem **7**, 1215 (2006).
[8] M. E. Gallagher, S. Haq, A. Omer, and A. Hodgson, Surf. Sci. **601**, 268 (2007).
[9] D. Sebastiani and L. Delle Site, J. Chem. Theory Comput. **1**, 78 (2005).
[10] M. Nakamura and M. Ito, Phys. Rev. Lett. **94**, 035501 (2005).
[11] M. Nakamura, M. Tanaka, M. Ito, and O. Sakata, J. Chem. Phys. **122**, 224703 (2005).
[12] G. Kresse and J. Furthmüller, Comput. Mater. Sci. **6**, 15 (1996).
[13] G. Kresse and D. Joubert, Phys. Rev. B **59**, 1758 (1999).
[14] J. P. Perdew, J. A. Chevary, S. H. Vosko, K. A. Jackson, M. R. Pederson, D. J. Singh, and C. Fiolhais, Phys. Rev. B **46**, 6671 (1992).
[15] D. R. Hamann, Phys. Rev. B **55**, R10157 (1997).
[16] C. Thierfelder, A. Hermann, P. Schwerdtfeger, and W. G. Schmidt, Phys. Rev. B **74**, 045422 (2006).
[17] F. Ortmann, W. G. Schmidt, and F. Bechstedt, Phys. Rev. Lett. **95**, 186101 (2005).
[18] F. Ortmann, F. Bechstedt, and W. G. Schmidt, Phys. Rev. B **73**, 205101 (2006).
[19] W. G. Schmidt, F. Bechstedt, and G. P. Srivastava, Phys. Rev. B **52**, 2001 (1995).